ISSN 1392-1320 MATERIALS SCIENCE (MEDŽIAGOTYRA). Vol. XX, No. X. 2025

The Application of IPMC Material Sensors in Collecting Flow Rates of Products

Meng Li *

Hubei Three Gorges Polytechnic, Yichang, 443000, China

http://doi.org/10.5755/j02.ms.37462

Received 28 May 2024; accepted 29 July 2024

With the rapid development of the economy and society, the demand for e-commerce products such as ocean speed sensors, heart rate sensors, and fingerprint recognition sensors is constantly increasing. This study selected an ion-exchange polymer metal composite (IPMC) with a certain potential for flow rate sensor applications to design experiments to test the performance of the flow rate sensor constructed with this material. As the density of the medium decreased, the deformation at the tip of the IPMC material decreased, and the pressure difference on the flow field cross-section increased. The densities of seawater and alcohol were 1072 kg/m^3 and 783 kg/m^3 respectively, with corresponding tip deformation and pressure difference of 0.20 mm and 0.14 mm, as well as 327 Pa and 86 Pa, respectively. As the temperature of seawater increased, the viscosity value of the medium decreased, and there was no significant change in the deformation and pressure difference at the tip of the corresponding IPMC. It indicates that within the range of changes in seawater viscosity, temperature has little effect on the deformation of IPMC, or in other words, IPMC has strong temperature adaptability under these conditions. When other conditions are the same, the larger the flow rate, the greater the deformation of IPMC. The experimental results demonstrate that under conditions of high length, width, and flow velocity, the IPMC flow velocity sensor designed in this study has high measurement accuracy. The research results contribute to the design of new IPMC flow rate sensors for e-commerce products.

Keywords: ion-exchange polymer metal composite, e-commerce, flow rate, sensors, voltage.

1. INTRODUCTION

In modern society, the rapid development of e-commerce has made online transactions feasible and efficient [1, 2]. At the same time, the maturity and development of fisheries have gradually increased the demand for high-performance flow velocity detectors among fishermen, whose core component is flow velocity sensors [3]. Therefore, if fishing companies and individuals want to improve production efficiency and reduce tool wear, it is necessary to obtain more practical and accurate flow velocity sensors. They are mainly used for flow velocity monitoring in sea areas, lakes, and other water bodies. Fishery entrepreneurs can analyze the movement patterns of fish schools, or the distribution of harsh ocean current environments based on measured data [4].

Ion exchange polymer metal composite (IPMC), as a new type of intelligent material, has excellent electrical and chemical properties. This material has excellent sensitivity, reaction rate, ductility, elasticity, and minimal heat transfer loss when in contact with a heat source, thus avoiding material damage caused by heat in traditional materials [5]. IPMC can also undergo significant deformation under current stimulation and generate corresponding electrical signals, which can provide a theoretical basis for implementing flow velocity sensors. In recent years, domestic and foreign experts and scholars have conducted extensive academic research to develop the performance of IPMC as a new material.

Researchers such as Annabetani have designed a microfluidic mixer based on an IPMC actuator to address the issue of low real-time detection efficiency in active microfluidic technology. By integrating the IPMC actuator into the microfluidic channel for detection, the results show that the mixer can effectively mix microfluidics [6]. To solve the problem that IPMC cannot provide both large deformation and fast response at the same time, scholars such as Ma designed a Nafion based IPMC composite material with high-quality metal electrodes. It was prepared by a new type of isopropanol assisted chemical plating, and the results showed that the material can achieve both large deformation and fast response at a high frequency AC voltage of 19 Hz [7]. Yang et al. proposed different thicknesses of IPMC composite materials based on solution casting technology to address the issue of the low output force of IPMC. The composite materials were prepared using Nafion520cs solution and chemical plating method. The results showed that the actuation performance of current transport through different thicknesses of IPMC under applied voltage was good [8]. He et al. developed a new type of liquid metal composite electrode at the beginning of the century to address the serious issues of electrode fatigue cracking and water loss in traditional IPMCs. The electrode used a mask to apply a liquid metal layer of eutectic gallium indium alloy (EGaIn) to the platinum electrode surface of IPMCs. The results showed that compared with the latest research, the fatigue strength of the composite electrode increased by 210 % [9]. To understand the physical basis of IPMC actuator driving, researchers such as Boldini tested hypotheses about the internal operation of IPMC driving in a new user unit through nonlinear finite element analysis. The results showed that the deformation through thickness has a high

* Corresponding author. Tel.: +86-0717-8853871; fax: +86-0717-8853871. E-mail: *limeng@htgp-edu.cn* (M. Li)

dependence on the double layer formed near the electrode [10]. Yin and other scholars added graphene dots to the IPMC actuator to further improve its driving performance. The results showed that after adding graphene dots, The working current, ion conductivity, blocking force, and needle tip displacement of IPMC are significantly improved [11].

In summary, many professionals have tested and optimized the performance of IPMC in different fields. However, most studies have applied IPMC to biomedical and biomimetic robots, with limited research on ocean velocity measurement. Therefore, by utilizing the sensing characteristics and good working ability of IPMC in humid environments, an innovative flow velocity sensor was designed and tested based on its flow velocity sensing characteristics. Through this study, it is expected to provide technical support for in-depth exploration of the marine world and sustainable development and utilization of marine resources.

This study is divided into four major parts. Part 1 is used to introduce IPMC materials and their potential applications in liquid flow velocity detection. Part 2 is designed for experimental testing of the performance and deformation patterns of IPMC flow velocity sensors. Part 3 conducts experiment and collects statistical experimental data. Part 4 analyzes the experimental data, summarizes the advantages and disadvantages of the experiment, and points out the direction for further research in the future.

2. MATERIALS AND METHODS

Flow velocity sensors are also a sales commodity on e-commerce platforms, which are used to obtain flow velocity data in fluid environments [12, 13]. IPMC has the potential to become a flow velocity sensor due to its advantages such as soft texture, lightweight, high sensitivity, and fast response speed [14]. Now, research is being conducted on the flow velocity sensing performance of IPMC, providing a reference for high-performance flow velocity sensors for e-commerce platforms.

2.1. Experimental design for analyzing the deformation characteristics of IPMC materials

To test whether IPMC material is suitable for preparing flow velocity sensors, it is necessary to study its deformation characteristics. Therefore, separate experiments are now designed to explore the relationship between deformation and flow rate, deformation and output voltage of IPMC materials. The IPMC used in the research institute is prepared through an impregnation of the reduction ion exchange process, including pretreatment, heat treatment, absorption, initial synthesis, secondary electroplating, and ion exchange. Firstly, sandblasting is used to roughen the surface of Nafion 117 and improve its surface adhesion. Then heat treat in an oven to bend the Nafion film. Next, exchange hydrophilic ion clusters (H^+) with platinum complex cations. Allow platinum ions to penetrate the given depth of Nafion film. Then, a platinum layer is formed on the surface of the original coating by a reduction method to improve the conductivity of the electrode. Finally, the H^+ in the IPMC membrane is exchanged with other counter ions such as Li^+ or Na^+ to obtain IPMC. The deformation of IPMC is achieved through the changes in ion flux inside the material and the drag effect of water molecules induced by ion migration [15, 16]. So, water content is an indicator that affects the performance of IPMC materials. It is now necessary to establish a response model under the action of an electric field to predict the macroscopic response and microscopic physical phenomena of IPMC materials under electrification. The physical properties of IPMC materials involved in this study can be segmented into four categories: material composition, microstructure, mechanical parameters, and electrical parameters. There is a relationship between them as shown in Fig. 1.

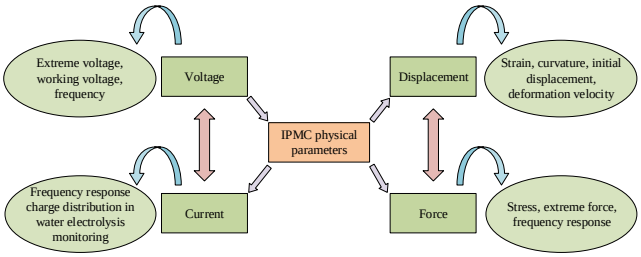

Fig. 1. Connection of four characteristics of IPMC materials

Construct a mechanical model based on a cantilever beam structure using IPMC material in the deformation characteristic experiment and fix a section on a copper electrode. The mechanical model is geometrically divided into a "free beam section" and a "clamping" section. To simulate these two parts, a mechanical model of IPMC material was constructed in ANSYS simulation software, based on a cantilever beam structure. Ensure that a portion of the model is fixed on the copper electrode to simulate the experimental setup. Divide the constructed mechanical model geometrically into two parts: free beam sections and clamping sections. Assign corresponding material properties to different parts after segmentation to ensure accurate reflection of the characteristics of IPMC materials in the simulation. Set the boundary conditions of the model to ensure that the clamping section remains fixed during the simulation process. Apply appropriate force or displacement to the "free beam segment" to simulate the bending process in the experiment. Run a simulation to observe the bending behavior of IPMC materials under the action of a force field. Record the changes in key parameters such as stress distribution and charge migration during the simulation process. If the IPMC material is only within the range of the force field and undergoes bending, the internal stress of the material will cause the migration of hydrated cations, resulting in a change in the distribution of charges. This is manifested as the potential difference between the upper and lower surfaces of the material, that is, a change in the output voltage *V*. In the experimental study on the relationship between deformation and flow velocity of IPMC designed in this article. Firstly, prepare multiple sets of IPMC samples based on the set dimensions, ensuring that the size and physical properties of each set of samples remain consistent to reduce experimental errors. Then build a fluid channel system with a controllable flow rate, accurately adjust the flow rate of the fluid (such as water) and monitor the flow rate changes in real time. Using high-precision displacement sensors and high-speed camera

technology, synchronously record the variation of IPMC deformation over time at different flow velocities. At the same time, gradually adjust the flow rate, conduct multiple gradient tests from low to high, and monitor fluid dynamics parameters, such as pressure distribution. Based on the actual application scenario conditions of IPMC, its dimensions are set as follows: length l = 30 mm, widths at both ends b_1 = 10 mm and b_2 = 5 mm, thickness h = 0.2 mm, elastic modulus E = 200 MPa, density ρ = 874 kg/m^3, and Poisson's ratio μ = 0.50. According to the above data, the rotation angle equation and deflection equation of IPMC material can be calculated, as shown in Eq. 1 and Eq. 2, respectively. The motion angle calculated by θ in Eq. 1

$$\theta = \frac{q}{6EI}(l-x)^3 - \frac{ql^3}{6EI}, \quad (1)$$

where I is the moment of inertia of the centroid axis of IPMC material; q is the surface load; x is the distance between the calculated object and the origin of rotation.

$$w = -\frac{qx^2}{24EI}(x^2 + 6l^2 - 4lx)^3, \quad (2)$$

where w is the calculated motion deflection.

This study sets the parameter setting scheme for deformation and flow rate testing of IPMC materials based on application scenarios and equipment conditions. The LabVIEW software was used to design the experimental control process to realize real-time acquisition and preliminary analysis of data. Experiment 1: in exploring the deformation of different media in the material flow field environment, the material dimensions were designed as 30 mm in length, 5 mm in width, and 0.2 mm in thickness, with a flow rate of 1 m/s and an ambient temperature of 25 ℃. The corresponding media schemes were seawater, alcohol, and oil, with densities of 1.07 × 10^3 kg/m^3, 7.85 kg/m^3, and 8.50 kg/m^3, and the condensation point of oil is generally lower than -20 ℃, which is related to the crystallization point of wax oil molecules in oil, respectively. Experiment 2: in the experiment to explore the effect of temperature on material deformation, the material size and environmental flow rate were set unchanged, and the temperature parameters were 5 ℃, 10 ℃, 15 ℃, 20 ℃, 25 ℃, and 30 ℃, respectively. Experiment 3: in the experiment to explore the influence of aspect ratio and flow direction angle on material deformation, the parameter setting schemes for each numbered sample are shown in Table 1.

Table 1. Parameter setting scheme for IPMC samples in Experiment 3

Parameter	#3_1	#3_2	#3_3	#3_4
Thickness, mm	0.20	0.20	0.20	0.20
Length, mm	30	30	30	30
Width, mm	5	10	10	10
Angle between sample and flow direction, °	90	90	60	30
Velocity of flow, m/s	0.01 ~10	0.01 ~10	0.01 ~10	0.01 ~10
Ambient temperature, ℃	25	25	25	25

ANSYS materials were used to analyze the distribution of deformation and load under different conditions. Before conducting the experiment, it was also necessary to use scanning electron microscopy to inspect the IPMC material itself.

This study also needs to explore the relationship between IPMC deformation and output voltage. Due to the actual application conditions, the thickness of IPMC material ranges from 0.3 mm to 0.8 mm, and the width is generally greater than 5 mm, which meets the morphological definition of thin plates. Therefore, this material can be treated as a thin plate material here, and the linear irreversible thermodynamic theory based on large deflection thin plates can be applied to analyze the deformation situation [17, 18].

2.2. Experimental design for performance study of IPMC sensors

The object of this experiment is still sheet shaped IPMC material, and the experimental platform architecture is shown in Fig. 2. The experimental platform consists of a water tank, IPMC material, data acquisition subsystem, clamping rod, horizontal linear motion platform, and aluminum alloy profile. The aluminum alloy profile is fixed on the horizontal linear motion platform by connecting parts. In the experimental platform, a clamping rod is used to connect the end of the aluminum alloy profile, thereby constructing a driving module. Considering the testing environment of the flow rate sensor, the motion speed range of the linear motion platform is set to 0 ~ 10 m/min. Since that the length of the water tank can affect the stability of the machine tool during movement, parameters of 0.1 m/s and 0.01 m/s are selected for the experiment.

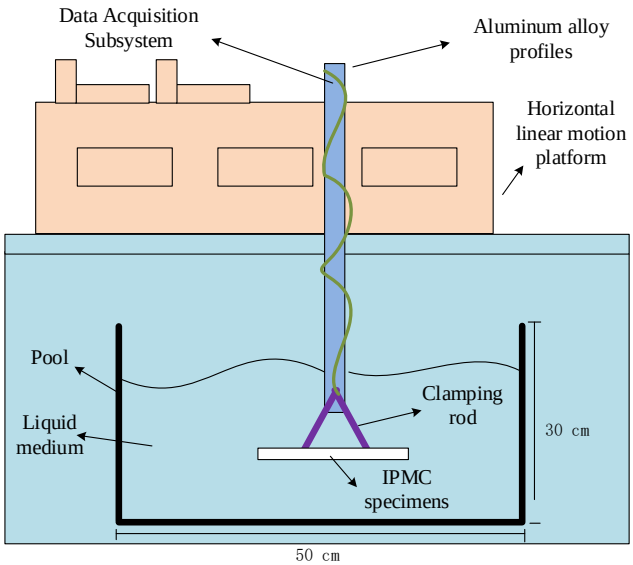

Fig. 2. Architecture of IPMC material sensor experimental platform

The clamping rod in the experimental platform will serve to place IPMC material in the cantilever structure and can also drive voltage. Considering that IPMC materials may contain leaked solvents, this study uses precious metals as electrical contacts to avoid oxidation and other types of conductivity deterioration. A high-precision data acquisition subsystem is constructed using a 24 bit

conversion chip and an STM32F105 micro-controller for the flow rate sensor experiment. Specifically, the converter in the data acquisition system includes a fourth-order incremental modulator and a programmable filter. This converter is of extremely low noise type and can support eight single ended inputs or four differential inputs as well as serial port download programs simultaneously. The reason for choosing the STM32F105 microcontroller model is that the controller has a smaller packaging volume. Compared with 8-bit microcontrollers, this type of micro-controller has a higher cost-effectiveness and can better meet the needs of this experiment.

In terms of software environment, this study adopts Keil software that supports the C language system as the software development environment. Compared to assembly language, C language has significant advantages in terms of readability, functionality, and maintenance difficulty. The overall framework of the program consists of initialization configuration, pin configuration, terminal configuration, serial port and interrupt response configuration, and data processing modules. During the system initialization process, it is necessary to first initialize the system's peripheral device clock and system clock, to initialize the peripheral devices. System initialization is a prerequisite for the normal operation of the entire experimental platform. After the experimental platform is powered on, the main program will first call the initialization program to complete the initial state setting of each hardware resource to ensure that each subroutine function can be maintained normally. In the system initialization phase, the first step is to configure the system clock, which is a prerequisite for other initialization configurations to proceed normally. The second step is to initialize the data analog-to-digital controller and the universal serial module. The third step is to initialize the advanced timer and peripheral interrupt controller. Serial communication software can play a role in sending measured displacement to the upper computer or other devices through the serial port, as well as receiving control instructions from other devices.

Fig. 3 shows the operational process of the data acquisition system required for the experimental platform. After the sensor transmits data to the A/D converter, the converter will perform preliminary processing on the data and upload it to the computer. The entire process requires a power supply.

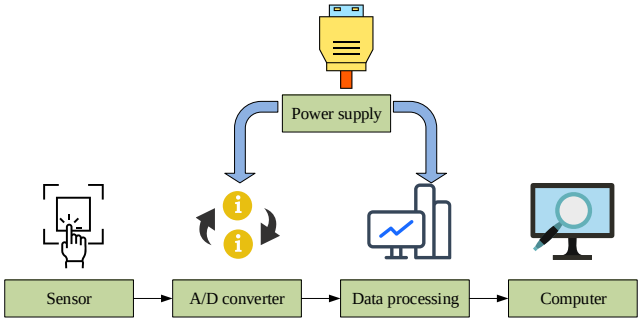

Fig. 3. Operation process of data collection system

Fig. 4 shows the software operation process of the data acquisition system. The system needs to be initialized before running, then the main program needs to be executed, and the voltage data needs to be repeatedly judged whether it has been transmitted. If it is determined as "yesto" convert the unit of data from the converter to "volts" and transfer the processed data to the computer.

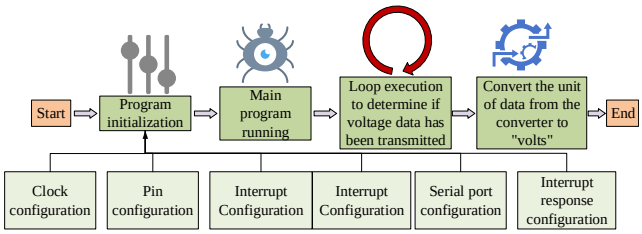

Fig. 4. Software operation process of data collection subsystem

The experimental conditions for conducting the sensing experiment of IPMC flow rate sensor are set, abbreviated as Experiment 4. The test objects used in Experiment 4 are two IPMC samples numbered #4_1 and #4_2. Their thickness, length, and width are 0.2 mm, 30 mm, 10 mm, and 0.2 mm, 30 mm, and 5 mm respectively. Samples #4_1 and #4_2 need to be tested at constant speeds of 0.01 m/s and 0.1 m/s respectively to collect their output voltage data. Each experimental protocol needs to be repeated 5 times to reduce the negative impact of irrelevant variables on the results. By analyzing the data collected in the experiment, the sensitivity, stability, repeatability, and range of IPMC material as a flow rate sensor can be determined.

Fig. 5 shows the overall experimental operation process of Experiment 4.

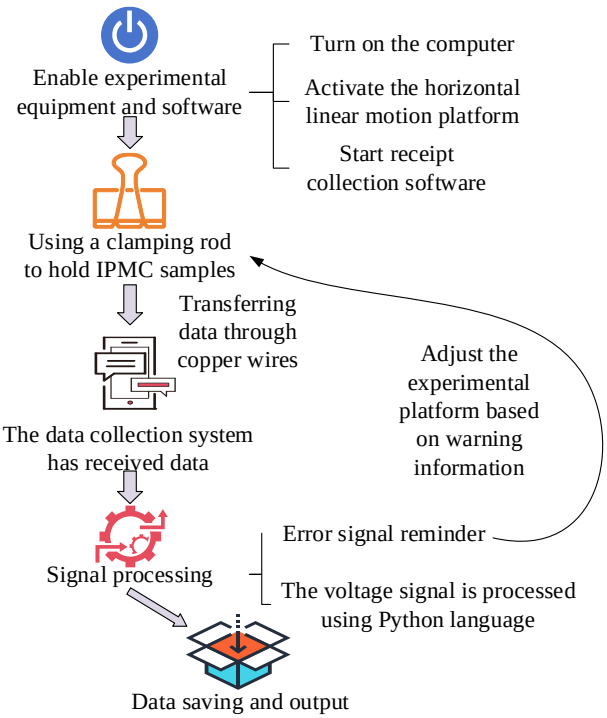

Fig. 5. Overall operation process of experiment 4

The first step is to start the horizontal linear motion platform and computer, and then open the data acquisition subsystem to set the required displacement, number of cycles, movement speed and other parameter values for the experiment. The second step is to use the lower part of the clamping rod to fix the IPMC material sample, and arrange copper sheets on the clamp, with wires soldered onto the copper sheets. This wire can conduct voltage data signals of

IPMC materials and transmit them to the data acquisition subsystem, thus forming a simple medium flow velocity sensor system. The third step is to enable the data collection subsystem to collect electrical signals. This should be first measured for a few seconds and observe that the IPMC sensor signal is stable before starting the horizontal linear motion platform. The purpose is to enable IPMC to move at the set speed, simulating the application scenario of flow rate sensors in e-commerce products. The final step is to save the obtained voltage signal in doc format and use Python language for data processing and processing to obtain fitting curve graphs under various conditions. Experiment 4 uses a clamping rod to fix the end of the aluminum alloy profile and IPMC material. The electrode signals on both sides of the material are connected to the signal conditioning circuit through a negative wire. The horizontal linear motion platform will drive the aluminum alloy profile and clamping rod to move along the guide rail. Moreover, the horizontal linear motion platform will change the flow velocity in the medium by setting the movement speed, thereby obtaining the sensing characteristic data of the IPMC transmission sensor.

This study conducted a series of experiments aimed at comprehensively evaluating the performance of IPMC materials as flow sensors. Firstly, by examining the physical properties, the thickness, length, and width of the IPMC film were verified to meet the experimental requirements, and its shape was checked for obvious damage or defects. Secondly, the microstructure of IPMC thin films was observed using scanning electron microscopy (SEM), and their fibrous structure and particle distribution were analyzed, as well as how these characteristics may affect their ion conductivity and mechanical strength. Furthermore, the performance of IPMC materials was tested under different media environments and environmental temperature conditions to investigate the effects of media density and temperature on the tip deformation and pressure difference of IPMC materials, and to evaluate their applicability under different media and environmental temperatures. In addition, performance tests were conducted on IPMC materials under different flow rate conditions to investigate the effect of flow rate on tip deformation and pressure difference of IPMC materials, and to evaluate their sensitivity and fatigue phenomena under different flow rate conditions. To gain a deeper understanding of the sensing performance of IPMC sensors, the flow velocity voltage relationship of the medium was also tested under different material media, aspect ratios, and flow angles. At the same time, a long-term experiment was conducted to test the performance of IPMC material sensors, to study the variation of output voltage with time when the IPMC sensor is in a uniform flow field environment for a long time, and to evaluate its stability and response time. Finally, the accuracy of the theoretical calculation method was evaluated by comparing theoretical and experimental values, and the effects of aspect ratio and flow velocity on sensor performance were studied, as well as the sensitivity of the sensor under these conditions.

3. RESULTS AND DISCUSSION

3.1. Experimental results of deformation characteristics analysis of IPMC materials

Fig. 6 shows the actual IPMC thin film after production. The thickness, length, and width of the IPMC sheet meet the experimental requirements, and there are no obvious damages or defects in the shape, which can be applied in Experiments 1 – 4.

Fig. 6. Physical image of IPMC thin film

Fig. 7 shows the images observed with the IPMC sheet scanning electron microscope (SEM) used in the experiment. The prepared IPMC sheets were dense and uniform in cross section with good material consistency. In Fig. 7 a, the thick end surface is slightly rough, with obvious fibrous structure and particles, which may be correlated with high ion transduction capacity and mechanical strength. However, in Fig. 7 b, the thin end surface is smoother, with less fibrous structure and particles, which may mean lower ion conduction capacity and mechanical strength. Both pictures are magnified at 100 micrometers to clearly show the microstructural differences between different parts of the IPMC material.

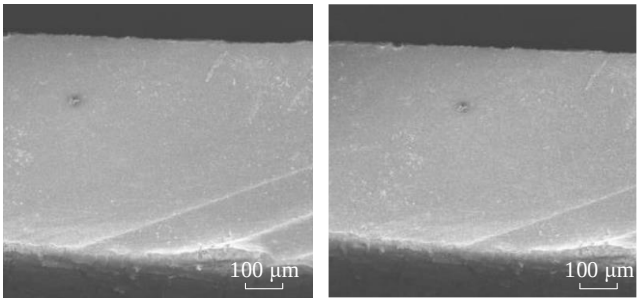

a b

Fig. 7. a – SEM observation results of the thick ends of IPMC flakes; b – SEM observation results of the thin ends of IPMC flakes

Now, following the commercial application standard to analyze the results of the IPMC experiments from the perspective of commercial applications and sensor performance. Fig. 8 shows the tip deformation and pressure

difference data of IPMC materials under different media environments and environmental temperature conditions.

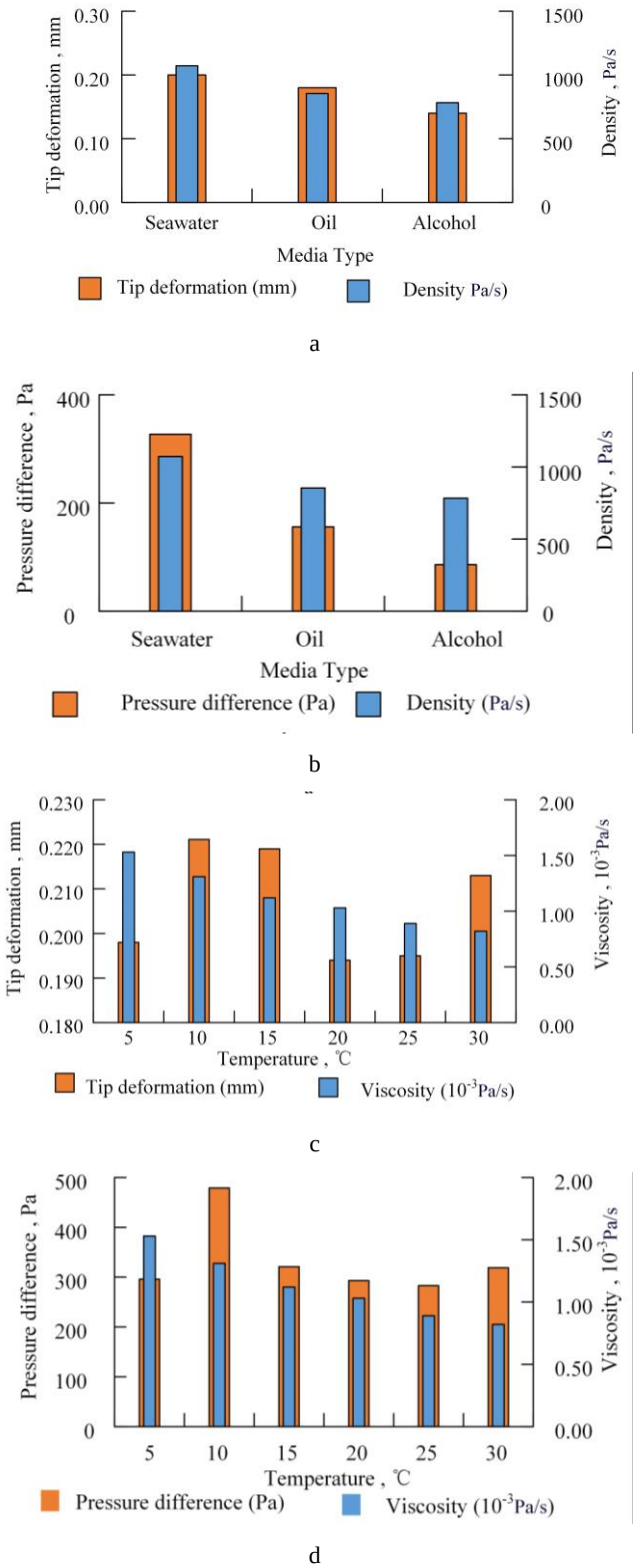

Fig. 8. a – the tip deformation data of IPMC under different media environments; b – the pressure difference data of IPMC under different media environments; c – the tip deformation data of IPMC under different temperature environments; d – the pressure difference data of IPMC under different temperature environments

As the medium density decreases, the deformation at the tip of the IPMC material decreases, while the pressure difference on the flow field cross-section increases. For example, the densities of seawater and alcohol are 1072 kg/m^3 and 783 kg/m^3 respectively, with corresponding tip deformations and pressure differences of 0.20 mm and 0.14 mm, as well as 327 Pa and 86 Pa, respectively. This indicates that IPMC is more sensitive to deformation in media with higher density. In Fig. 8 b, as the seawater temperature increases, the viscosity value of the seawater decreases, and the corresponding IPMC tip deformation and pressure difference do not show significant changes. This indicates that within the range of changes in seawater viscosity, temperature has little effect on the deformation of IPMC, or in other words, IPMC has strong temperature adaptability under these conditions.

Table 2 shows the tip deformation and pressure difference data of IPMC materials under different flow velocity conditions. As the aspect ratio of IPMC increases, the material deformation under the same flow field conditions increases. In this case, if the flow rate is not less than 1 m/s, the aspect ratio increases and the pressure difference also increases. This indicates that the sensitivity of IPMC materials is higher when the aspect ratio is large. In addition, under the same conditions, the larger the flow rate, the greater the deformation of IPMC. For example, when the flow velocity is 0.01 m/s, 0.10 m/s, 1.00 m/s, and 10.00 m/s, the deformation of #3_1 is 1.551×10^{-3} mm, 8.741×10^{-3} mm, 0.1496 mm, and 18.47 mm, respectively. This indicates that IPMC materials have higher sensitivity in larger flow fields, but at the same time, they are more likely to experience fatigue phenomena.

Table 2. Tip deformation and pressure difference data of IPMC material under different flow velocity conditions

Medium flow velocity, m/s	Material number	Cross-section pressure difference in flow field, Pa	Tip deformation, mm
0.01	#3_1	38.86	1.551×10^{-3}
	#3_2	167.9	1.501×10^{-3}
	#3_3	1.816	1.148×10^{-4}
	#3_4	0.542	8.902×10^{-5}
0.10	#3_1	108.2	8.741×10^{-3}
	#3_2	237.9	6.782×10^{-3}
	#3_3	4.486	2.593×10^{-3}
	#3_4	5.096	1.774×10^{-3}
1.00	#3_1	379.2	0.1496
	#3_2	288.4	9.335×10^{-2}
	#3_3	249.1	0.1185
	#3_4	324.5	0.1321
10.00	#3_1	2.856×10^4	18.47
	#3_2	2.693×10^4	10.05
	#3_3	2.364×10^4	11.47
	#3_4	3.261×10^4	13.22

Fig. 9 shows the flow velocity voltage data of the medium under different material media, aspect ratios, and flow direction angles. There is little difference in the relationship between flow velocity and material voltage in media with different densities. When there is a smaller aspect ratio and other conditions are the same, the voltage fluctuation of the IPMC sensor is greater. For example,

when the flow rate is 1.00 m/s and the aspect ratio is 6, the material output voltage of the 3 schemes is 23.8 mV and 15.4 mV, respectively.

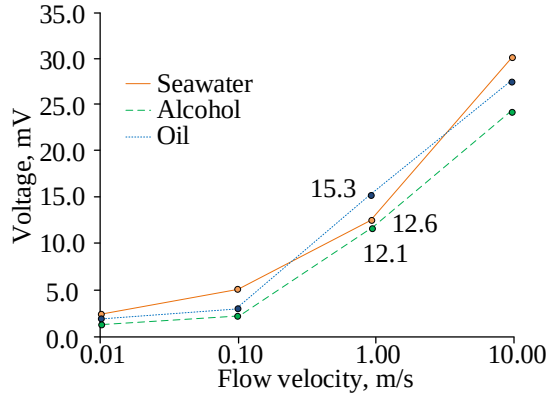

a

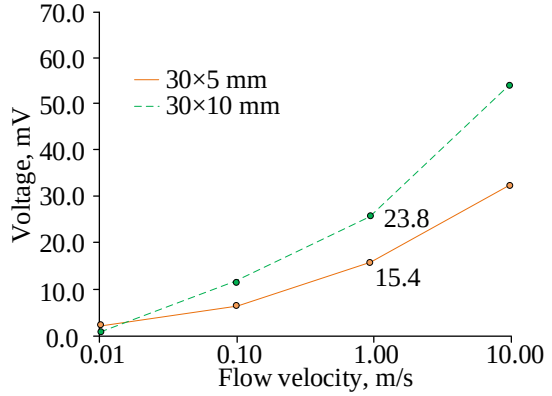

b

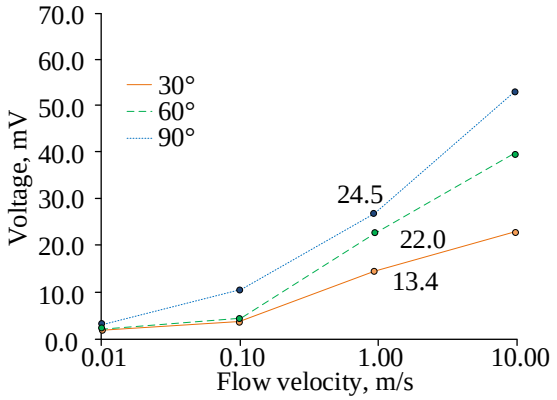

c

Fig. 9. a – the relationship between medium flow velocity and voltage under different material media; b – the relationship between medium flow velocity and voltage under different material aspect ratios; c – the relationship between medium flow velocity and voltage under different flow direction angles

In Fig. 9 c, when other conditions are the same, the larger the angle between the flow directions, the greater the amplitude of the change in the output voltage value of the sensor. The points on the curve in the first chart represent the voltage readings at a specific fluid flow velocity. For example, "15.3", "12.6", and "12.1" correspond to voltage values of a specific fluid flow velocity. The points on the second chart curve represent the voltage readings at a specific fluid flow velocity. Values such as "23.8" and "15.4" are voltage values corresponding to a specific fluid flow velocity. The third chart has three curves representing three different flow angles (30°, 60°, and 90°). The points here also represent voltage readings at specific fluid flow speeds. The values of "24.5", "22.0", "13.4", etc. are the voltage values corresponding to the fluid flow velocity.

The research focuses on the potential application of IPMC (Ionic Polymer Metal Composite) thin films in e-commerce flow sensors, and its performance is analyzed in depth through a series of experiments. The experimental results showed that the prepared IPMC film met the experimental requirements in terms of physical morphology. SEM images showed its dense and uniform microstructure, but there were differences in fibrous structure and particle distribution between the thick and thin ends, suggesting different ion conductivity and mechanical strength. In tests under different media environments and temperature conditions, IPMC exhibits higher deformation sensitivity and good temperature adaptability to high-density media. In addition, the sensitivity of IPMC increases with the increase of aspect ratio and flow rate, but it is also more prone to fatigue. The relationship between flow rate and voltage is less affected by the density of the medium, while changes in aspect ratio and flow direction angle have a significant impact on the output voltage of the sensor. These findings provide important references for the commercial application of IPMC in the field of flow sensing.

3.2. Experimental results of IPMC material sensor performance testing

Fig. 10 shows the variation data of the output voltage of each group of sensors over time obtained from Experiment 4. The dashed lines of different colors in Fig. 10 represent the optimal fitting curves for the corresponding color flow rate groups. Its R^2 value was calculated to be 0.964 and significantly higher than the other experimental groups. The equation shown in Fig. 10 is the corresponding optimal fitting equation. When the IPMC sensor is in a uniform flow field environment, as time progresses, the output voltage shows a pattern of rapid growth first, and then tends to stabilize. But the higher the medium flow rate, the higher the stable output voltage. After the experimental time exceeded 50 seconds, the data of all experimental groups reached a stable state.

Fig. 11 shows the error between the theoretical calculated value and the experimental value of the output voltage. The horizontal axis in the picture. Fig. 11 a is the aspect ratio and medium flow velocity of the IPMC sample, with the flow velocity unit being m/s. The left vertical axis represents the theoretical output voltage value and the experimental output voltage value. Fig. 11 b shows the percentage error of the theoretical output voltage value relative to the experimental value. The percentage error in the above content refers to the degree of deviation between the theoretical output voltage value and the experimental output voltage value, used to quantify the difference between theoretical calculations and experimental measurements.

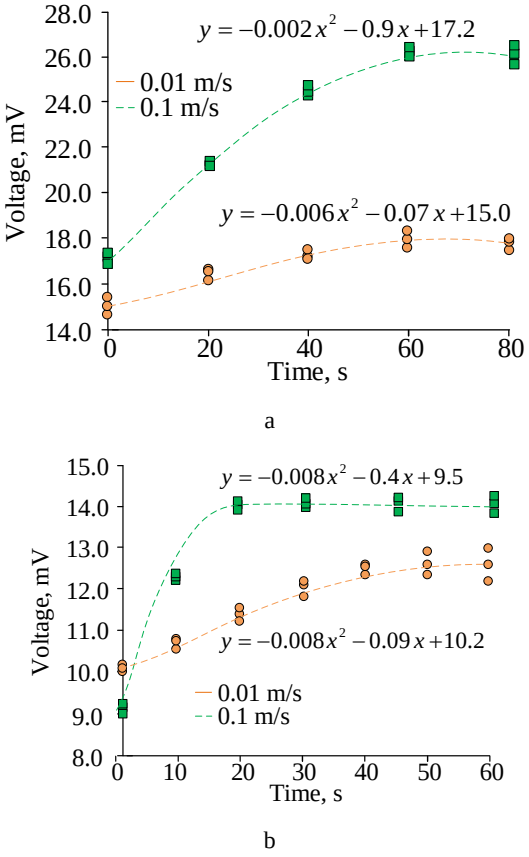

Fig. 10. Output voltage time data for each sensor group: a – sample #4_1; b – Sample #4_2)

The calculation process usually involves the following steps: first, calculate the difference between the theoretical output voltage value and the experimental output voltage value; Secondly, divide this difference by the experimental output voltage value to obtain the relative error; Finally, multiply this relative error by 100 % and convert it into percentage form to more intuitively express the magnitude of the error. The smaller the percentage error, the closer the theoretical calculation value is to the experimental value, and the better the performance of the sensor. Conversely, the smaller the percentage error, the greater the deviation between the theoretical calculation and experimental measurement. Using a box plot to describe the distribution of data obtained from parallel experiments and using dots to represent relative errors. Under the same medium flow rate conditions, the larger the aspect ratio of IPMC material, the smaller the error between the theoretical and experimental values of sensor voltage. When the flow velocity is 0.1 m/s and the aspect ratio is 3.0 and 6.0, the relative errors are 55.8 % and 8.1 %, respectively. Under the same aspect ratio conditions, the higher the medium flow rate, the smaller the relative error of the sensor. When the aspect ratio is 6.0, the relative errors of data with flow velocities of 0.01 m/s and 0.1 m/s are 13.2 % and 8.1 %, respectively. In summary, this study found through experiments on IPMC flow rate sensor equipment that under conditions of large aspect ratio and high flow rate, the designed theoretical calculation method has a smaller error compared to the actual value, and the sensitivity of the sensor is higher. In summary, an in-depth experimental analysis was conducted on the IPMC (Ionic Polymer Metal Composite) flow sensor, with a focus on examining its output voltage characteristics under different conditions.

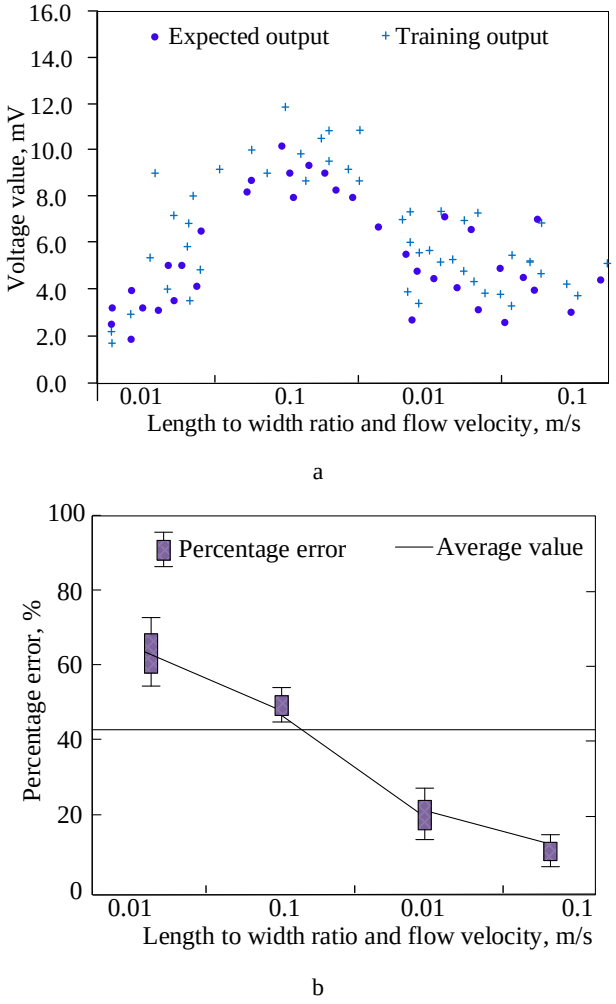

Fig. 11. Error comparison between theoretical calculated value and experimental value of output voltage: a – changes in voltage value; b – change in percentage error

The experimental results show that when the IPMC sensor is placed in a uniform flow field environment, its output voltage shows a pattern of rapid growth followed by stabilization over time, and the higher the medium flow rate, the higher the stable output voltage. In addition, by comparing the theoretically calculated values with the experimental output voltage values, it was found that there is a certain degree of error between the two, but this error is significantly reduced under larger aspect ratios and high flow conditions, indicating that the performance of the sensor is better under these conditions, and the accuracy of the theoretical calculation method has also been improved.

3.3. Discussion of experimental results

The material of deformable sensors has a significant impact on their performance. The physical and SEM images of IPMC thin films in this study show that there are no obvious structural defects or uneven material distribution in the material itself. This ensures the reliability of subsequent experimental results and eliminates errors caused by material defects. In previous studies, many scholars have made significant breakthroughs in the deformation

mechanism of IPMC materials. The study by Omiya et al. suggests that the deformation mechanism of IPMC depends on the applied voltage, electrode thickness, and actuator thickness. The influence of the medium on the bending deformation of IPMC with shorter and thinner electrodes is greater [19]. In this study, IPMC is more sensitive to deformation in media with higher density. This is because under the same flow rate conditions, a medium with higher density will bring greater contact surface pressure to the IPMC material. This pressure is the core cause of material deformation under stress. Similarly, temperature changes in liquid media do not directly or indirectly affect the contact surface pressure on IPMC materials, and therefore cannot affect the deformation patterns of the materials. This discovery can well explain the results obtained by Omiya et al. Zhang et al. found that when the transverse and longitudinal dimensions of the material were small, IPMC produced a displacement of 0.26 mm [20]. In this study, it was found that under the same medium flow rate conditions, the larger the aspect ratio of IPMC material, the smaller the error between the theoretical and experimental values of sensor voltage. This result is like the results of Zhang et al. This is because as the aspect ratio of the material increases, the length direction deformation generated by the material is less affected by the unstable flow of local medium pressure, and the output voltage data can be closer to the real data. However, the limitation of this study is that it did not allow potential customers of flow rate sensor e-commerce products to test and subjectively evaluate the undesigned sensors. This may affect the difficulty of marketization for such products.

4. CONCLUSIONS

This study designed experiments to test the performance of the flow velocity sensor constructed with this material, as well as the flow velocity deformation law of IPMC material. The test results showed that the thickness, length, and width of the IPMC sheet met the experimental requirements, and there were no obvious damages or defects in the appearance. The IPMC thin slice produced had a dense and uniform micro-structure on the transverse section, with good material consistency. The generated electrical signal was not affected by structural defects in the material itself and was suitable for designing medium flow rate sensors. As the density of the medium decreased, the deformation at the tip of the IPMC material decreased, while the pressure difference on the flow field cross-section increased. The densities of seawater and alcohol were 1072 kg/m^3 and 783 kg/m^3 respectively, with corresponding tip deformation and pressure difference of 0.20 mm and 0.14 mm, as well as 327 Pa and 86 Pa, respectively. This indicates that IPMC is more sensitive to deformation in media with higher density. As the temperature of seawater increased, the viscosity value of seawater decreased, and the corresponding IPMC tip deformation and pressure difference did not show significant changes. This indicates that within the range of changes in seawater viscosity, temperature has little effect on the deformation of IPMC, or in other words, IPMC has strong temperature adaptability under these conditions. When other conditions were the same, the larger the flow rate, the greater the deformation of IPMC. When the aspect ratio was small and other conditions were the same, the voltage fluctuation of IPMC sensors was greater. When other conditions were the same, the larger the flow angle, the greater the amplitude of the output voltage value of the sensor. As time went on, the output voltage showed a pattern of rapid growth first and then stabilizing, but the higher the medium flow rate, the higher the stable output voltage.

REFERENCES

1. **Zhang, Y., Srimuk, P., Aslan, M., Gallei, M., Presser, V.** Polymer Ion-Exchange Membranes for Capacitive Deionization of Aqueous Media with Low and High Salt Concentration *Desalination* 479 (7) 2020: pp. 114331.1 – 114331.10. https://doi.org/10.1016/j.desal.2020.114331
2. **Voropaeva, D.Y., Novikova, S.A., Yaroslavtsev, A.B.** Polymer Electrolytes for Metal-Ion Batteries *Russian Chemical Reviews* 89 (10) 2020: pp. 1132 – 1155. https://doi.org/10.1070/RCR4956
3. **Markvart, A.A., Liokumovich, L.B., Medvedev, I.O., Ushakov, N.A.** Smartphone-Based Interrogation of a Chirped FBG Strain Sensor Inscribed in a Multimode Fiber *Journal of Lightwave Technology* 39 (1) 2020: pp. 282 – 289. https://doi.org/10.1109/JLT.2020.3024713
4. **Murali, G., Reddeppa, M., Reddy, C.S., Park, S., Chandrakalavathi, T., Kim, M., In, I.** Enhancing the Charge Carrier Separation and Transport via Nitrogen Doped Graphene Quantum Dot-TiO_2 Nanoplate Hybrid Structure for Efficient NO Gas Sensor *ACS Applied Materials & Interfaces* 12 (11) 2020: pp. 13428 – 13436. https://doi.org/10.1021/acsami.9b19896
5. **Aubry, A., Braca, P., Maio, A.D., Marino, A.** Enhanced Target Localization with Deployable Multiplatform Radar Nodes Based on Non-Convex Constrained Least Square Optimization *IEEE Transactions on Signal Processing* 70 2021: pp. 1282 – 1294. https://doi.org/10.48550/arXiv.2104.11209
6. **Annabestani, M., Azizmohseni, S., Esmaeili-Dokht, P., Bagheri, N., Aghassizadeh, A., Fardmanesh, M.** Multiphysics Analysis and Practical Implementation of a Soft μ-Actuator- Based Microfluidic Micromixer *Journal of Microelectromechanical Systems* 29 (2) 2020: pp. 268 – 276. https://doi.org/10.1109/JMEMS.2020.2975560
7. **Ma, S., Zhang, Y., Liang, Y., Ren, L., Tian, W.J., Ren, L.Q.** High-Performance Ionic-Polymer-Metal Composite: Toward Large-Deformation Fast-Response Artificial Muscles *Advanced Functional Materials* 30 (7) 2020: pp. 1908508.1 – 1908508.9. https://doi.org/10.1002/adfm.201908508
8. **Yang, L., Zhang, D., Zhang, X., Tian, A., He, M.M.** Property of Ionic Polymer Metal Composite with Different Thicknesses Based on Solution Casting Technique *International Journal of Modern Physics B* 34 (28) 2020: pp. 2050263.1 – 2050263.10. https://doi.org/10.1142/S021797922050263X
9. **He, Z., Jiao, S., Wang, Z., Wang, Y., Yang, M., Zhang, Y., Liu, Y., Wu, Y., Shang, J., Chen, Q., Li, R.W.** An Antifatigue Liquid Metal Composite Electrode Ionic Polymer-Metal Composite Artificial Muscle with Excellent Electromechanical Properties *ACS Applied Materials & Interfaces* 14 (12) 2022: pp. 14630 – 14639. https://doi.org/10.1021/acsami.2c01453

10. **Boldini, A., Porfiri, M.** Multiaxial Deformations of Ionic Polymer Metal Composites *International Journal of Engineering Science* 149 2020: pp. 103227.1 – 103227.28. https://doi.org/10.1016/j.ijengsci.2020.103227
11. **Yin, G., He, Q., Yu, M., Wu, Y.W., Xu, X.R.** Ionic Polymer Metal Composites Actuators with Enhanced Driving Performance by Incorporating Graphene Quantum Dots *Journal of Central South University* 29 (5) 2022: pp. 1412 – 1422. https://doi.org/10.1007/s11771-022-5040-7
12. **Wang, Y., Ji, H., Zhang, X., Shi, J., Li, X., Jiang, X., Qu, X.** Cyclopropenium Cationic-Based Covalent Organic Polymer-Enhanced Poly(ethylene oxide) Composite Polymer Electrolyte for All-Solid-State Li–S Battery *ACS Applied Materials & Interfaces* 13 (14) 2021: pp. 16469 – 16477. https://doi.org/10.1021/acsami.1c02309
13. **Shi, P., Ma, J., Huang, Y., Fu, W., Li, S., Wang, S., Zhang, D., He, Y., Kang, F.** A Thin and High-Strength Composite Polymer Solid-State Electrolyte with a Highly Efficient and Uniform Ion-Transport Network *Journal of Materials Chemistry A* 9 (25) 2021: pp. 14344 – 14351. https://doi.org/10.1039/D1TA03059K
14. **Xia, Y., Xu, N., Du, L., Cheng, Y., Lei, S., Li, S., Liao, X., Shi, W., Xu, L.** Rational Design of Ion Transport Paths at the Interface of Metal-Organic Framework Modified Solid Electrolyte *ACS Applied Materials & Interfaces* 12 (20) 2020: pp. 22930 – 22938. https://doi.org/10.1021/acsami.0c04387
15. **Wu, J.L., Zhang, Z.D., Huang, H.T., Gao, X., Xu, J., Wang, S.** Polymer Thin Film Memtransistors Based on Ion-Carrier Exchange Heterojunction *IEEE Electron Device Letters* 42 (10) 2021: pp. 1528 – 1531. https://doi.org/10.1109/LED.2021.3103774
16. **Kmiec, S., Ruoff, E., Darga, J.** Scalable Glass-Fiber-Polymer Composite Solid Electrolytes for Solid-State Sodium-Metal Batteries *ACS applied Materials & Interfaces* 15 (17) 2023: pp. 20946 – 20957. https://doi.org/10.1021/acsami.3c00240
17. **Chen, H., Zhou, C.J., Dong, X.R., Yan, M., Liang, J.Y., Xin, S., Wu, X., Guo, Y., Zeng, X.** Revealing the Superiority of Fast Ion Conductor in Composite Electrolyte for Dendrite-Free Lithium-Metal Batteries *ACS Applied Materials & Interfaces* 13 (19) 2021: pp. 22978 – 22986. https://doi.org/10.1021/acsami.1c04115
18. **He, X., Ye, A., Fu, X., Yang, W., Yu, W.** Achieving Low-Energy-Barrier Ion Hopping in Adhesive Composite Polymer Electrolytes by Nanoabsorption *Macromolecules* 55 (16) 2022: pp. 7117 – 7126. https://doi.org/10.1021/acs.macromol.2c00928
19. **Omiya, M., Kurokawa, M.** Deformation mechanism of hydrogen-assisted ionic polymer metal composite actuator *Mechanics of Advanced Materials and Structures* 30 (2) 2023: pp. 225 – 235. https://doi.org/10.1080/15376494.2021.2011990
20. **Zhang, T., Chen, K., Wu, J.** Deformation Performance of Pt-IPMC Based on Experiment and Simulation Research *Integrated Ferroelectrics* 232 (1) 2023: pp. 19 – 28. https://doi.org/10.1080/10584587.2023.2173439